







## Article

# An Ancient Egyptian Multilayered Polychrome Wooden Sculpture Belonging to the Museo Egizio of Torino: Characterization of Painting Materials and Design of Cleaning Processes by Means of Highly Retentive Hydrogels

Nicole Manfreda <sup>1</sup>, Paola Buscaglia <sup>1,\*</sup>, Paolo Gallo <sup>2</sup>, Matilde Borla <sup>3</sup>, Sara Aicardi <sup>4</sup>, Giovanna Poggi <sup>5</sup> , Piero Baglioni <sup>5</sup> , Marco Nervo <sup>1,9</sup> , Dominique Scarone <sup>7</sup> , Alessandro Borghi <sup>8</sup>, Alessandro Re <sup>6,9</sup> , Laura Guidorzi <sup>6,9</sup>  and Alessandro Lo Giudice <sup>6,9</sup>

- <sup>1</sup> Centro Conservazione e Restauro la Venaria Reale, 10078 Venaria Reale, Italy; nicole.manfreda@edu.unito.it (N.M.); marco.nervo@centrorestaurovenaria.it (M.N.)
  - <sup>2</sup> Dipartimento di Studi Storici, Università di Torino, 10124 Torino, Italy; p.gallo@unito.it
  - <sup>3</sup> Soprintendenza Archeologia, Belle Arti e Paesaggio per la città Metropolitana di Torino, 10124 Torino, Italy; matilde.borla@beniculturali.it
  - <sup>4</sup> Museo Egizio di Torino, 10124 Torino, Italy; sara.aicardi@museoegizio.it
  - <sup>5</sup> Dipartimento di Chimica and CSGI, Università di Firenze, 50019 Sesto Fiorentino, Italy; poggi@csgi.unifi.it (G.P.); baglioni@csgi.unifi.it (P.B.)
  - <sup>6</sup> Dipartimento di Fisica, Università di Torino, 10124 Torino, Italy; alessandro.re@unito.it (A.R.); laura.guidorzi@unito.it (L.G.); alessandro.logiudice@unito.it (A.L.G.)
  - <sup>7</sup> Dipartimento di Chimica, Università di Torino, 10124 Torino, Italy; dominique.scalarone@unito.it
  - <sup>8</sup> Dipartimento di Scienze della Terra, Università di Torino, 10124 Torino, Italy; alessandro.borghi@unito.it
  - <sup>9</sup> Istituto Nazionale di Fisica Nucleare, Sezione di Torino, 10124 Torino, Italy
- \* Correspondence: paola.buscaglia@centrorestaurovenaria.it; Tel.: +39-011-499-3060



**Citation:** Manfreda, N.; Buscaglia, P.; Gallo, P.; Borla, M.; Aicardi, S.; Poggi, G.; Baglioni, P.; Nervo, M.; Scarone, D.; Borghi, A.; et al. An Ancient Egyptian Multilayered Polychrome Wooden Sculpture Belonging to the Museo Egizio of Torino: Characterization of Painting Materials and Design of Cleaning Processes by Means of Highly Retentive Hydrogels. *Coatings* **2021**, *11*, 1335. <https://doi.org/10.3390/coatings11111335>

Academic Editor: Robert J. K. Wood

Received: 11 September 2021

Accepted: 15 October 2021

Published: 30 October 2021

**Publisher's Note:** MDPI stays neutral with regard to jurisdictional claims in published maps and institutional affiliations.



**Copyright:** © 2021 by the authors. Licensee MDPI, Basel, Switzerland. This article is an open access article distributed under the terms and conditions of the Creative Commons Attribution (CC BY) license (<https://creativecommons.org/licenses/by/4.0/>).

**Abstract:** This contribution focuses on the conservation of an Egyptian wooden sculpture (Inventory Number Cat. 745) belonging to the Museo Egizio of Torino in northwest Italy. A preliminary and interdisciplinary study of constituent painting materials and their layering is here provided. It was conducted by means of a multi-technique approach starting from non-invasive multispectral analysis on the whole object, and subsequently, on selected micro-samples. In particular, visible fluorescence induced by ultraviolet radiation (UVF), infrared reflectography (IRR) and visible-induced infrared luminescence were used on the whole object. The micro-samples were analysed by means of an optical microscope with visible and UV light sources, a scanning electron microscope (SEM) with an energy-dispersive X-ray spectrometer (EDX), Fourier transform infrared (FT-IR) spectrometer, pyrolysis-gas chromatography/mass spectrometer (Py-GC/MS) and micro-particle induced X-ray emission (PIXE). The characterization of the painting materials allowed the detection of Egyptian blue and Egyptian green, and also confirmed the pertinence of the top brown layer to the original materials, which is a key point to design a suitable surface treatment. In fact, due to the water sensitiveness of the original materials, only few options were available to perform cleaning operations on this artwork. To setup the cleaning procedure, we performed several preliminary tests on mockups using dry cleaning materials, commonly used to treat reactive surfaces, and innovative highly water retentive hydrogels, which can potentially limit the mechanical action on the original surface while proving excellent cleaning results. Overall, this study has proved fundamental to increase our knowledge on ancient Egyptian artistic techniques and contribute to hypothesize the possible provenance of the artefact. It also demonstrated that polyvinyl alcohol-based retentive gels allow for the safe and efficient cleaning of extremely water sensitive painted surfaces, as those typical of ancient Egyptian artefacts.

**Keywords:** cultural heritage; conservation; wooden sculpture; ancient Egyptian; ancient Egyptian painting materials; cleaning treatment; water based systems; poly(vinyl alcohol) hydrogels; archaeometry

## 1. Introduction

Designing a correct conservation treatment process requires an interdisciplinary work that involves professionals from various fields, in order to combine and incorporate several approaches and data to reach an overview, as complete as possible, of the artefact. In particular, for archaeological objects, besides notes on the specific excavation activities, few documented information are available on the artistic techniques and conservation history. In this context, archaeometric studies do strongly contribute to the study of archaeological finds.

This paper focuses on the study of an Egyptian wood sculpture dating back to New Kingdom (1550–1069 B.C.E.), which belongs to the Museo Egizio of Torino (Inventory Number Cat. 745). In particular, the characterization of painting materials and the set-up of an adequate cleaning treatment of the surface of the sculpture are here provided.

The Cat. 745 statuette represents Hapy, god of the Nile flood, or a more generic fecundity figure, and seems to be the only known case, until now, of a wooden sculpture depicting this subject (Figure 1). The figure is standing, placed on a rectangular base, with the left feet ahead. It is missing of his forearms that probably held an offering table, in consideration of both the morphology of joints and of the common iconography of these figures. It is represented with a wig and dressed only with a belt fixed on the hips, characterized by three long stripes up to the knees. This type of figures often has an insignia on their head representing their name but, in this case, this feature is missing, making impossible to ascertain the specific representation [1].



**Figure 1.** Inventory Number Cat. 745 before the cleaning treatment. Measurements (h × w × d) 62 cm × 16 cm × 25.5 cm. (a): front side, diffuse light. (b): back side, diffuse light.

The statuette was studied from 2005 to 2007 within the framework of three Bachelor theses [2–4] and, later (2017–2019), in the framework of a Master dissertation [5], which focused on conservation treatments. Taking into account the unusual multi-layered polychromies, scientific insights have been provided, in order to characterize both pigments and binders for a better comprehension of the artistic technique. Moreover, it appeared necessary to detect the presence of non-original materials, in the view of setting up a cleaning treatment, for a proper reading of the decoration of the statuette.

A brief description of the case study and of its layering of materials seems necessary to understand the aim of the research process.

In terms of painted decoration, the artefact presents, by a visual inspection, multi-layered polychromies, alternating ground layers and coloured layers. Specifically, in the body and wig parts of the sculpture five layers of materials are present (Figure 2), two of which refer to preparation layers (in Figure 2, starting from the interface with the wooden material, layer 1 and layer 3), while the other three correspond to paint layers.



**Figure 2.** Scheme of the layer sequence in painting materials in the wig (a) and in the body (b) of the sculpture. The thickness of the layers is not in scale.

Having no information about the history of the object before its arrival in Torino, we could only presume that it was acquired between 1824 and 1882, the year in which it is described in a catalogue [6], with the inventory number (745) and its original location. Few information is also available about its conservation history. Archive black & white photos dating back to the 1970s were retrieved; they showed a thick layer of dust, visible in particular on the upper face of the base. In addition to this, the only documented report on a securing treatment carried on the artefact by Luigi Vigna, at that time director of the conservation laboratory of the Museo Egizio, was found [2–4]. In this context, the removal of the dust and the consolidation of the preparation and paint were carried out, with the aim of allowing a correct reading and a safe handling of the object. Further maintenance interventions, which are difficult to place chronologically have been indeed carried out: for instance a modern nail inserted to reinforce the assembly of the arm was clearly detected by X-ray radiography (not shown here).

Considering the complex layering of materials, it was necessary to understand if the cleaning operations had to be limited to the surface dirt, or if the removal of one or

more paint layers might be considered, if these were demonstrated to be non-original. In particular, the characterization of the brown top layer seemed necessary: even if not visible near to the gaps, and therefore, apparently not applied after some deterioration, without more information on its nature, it was not possible to exclude in advance its pertinence to a non-original patina. Moreover, it is worth noting that the superficial dirt was placed on top of a rough, porous and extremely fragile surface, which could have made the cleaning operation particularly challenging (Figure 3).



**Figure 3.** Detail of the back of the case study. It can be seen that different paint layers are covered with dust.

Archaeological painting materials as the Egyptian ones, are often strongly water-sensitive, and cannot be cleaned with traditional gels such as agarose-based ones. However, in consideration of the lack of superficial cohesion of the materials, any mechanical action, as that associated with dry cleaning methods, might have been too stressful for the surface. Therefore, it was decided to compare traditional dry-cleaning methods, widely tested and commonly used on archaeological polychromies [7], with innovative highly retentive water-based hydrogels, recently introduced in conservation practice [8–10]. In particular, among the available formulations, it was decided to test twin-chain polymer hydrogels based on poly(vinyl alcohol), which have been developed for the cleaning of water-sensitive modern and contemporary artworks [11–14]. These systems, which, to the best of our knowledge, have not been previously tested on ancient Egyptian artefacts, combine good adhesion to rough and textured paint layers, and controlled wetting of surfaces, granting safe removal of soil. The combination of dry-cleaning materials with highly retentive gels was expected to grant a delicate and localized action at the interface with the original paint layer.

## 2. Materials and Methods

### 2.1. Painting Materials Analysis

To identify the used pigments and to study the complex structure of painting materials, an approach based on non-invasive and micro-invasive techniques approach in a two-step sequence was applied as provided in standard protocols for conservation purposes [15], starting from non-invasive multispectral analysis on the whole object, and subsequently, on selected samples.

For the characterization of painting materials three typologies of non-invasive analysis techniques were employed: visible fluorescence induced by ultraviolet radiation (UVF), infrared reflectography (IRR) and visible-induced infrared luminescence (VIL). UVF is useful for the identification of different materials on the surface which are not easily discerned using visible light, including previous conservation treatments. IRR uses the near infrared to investigate under the paint layers and to highlight the potential presence of preparatory drawings or other pictorial materials. Moreover, it can be combined with visible light photographs to produce false colour (IRFC) images, which can be used to tentatively identify pigments. Finally, the VIL technique is mainly used to identify the presence of Egyptian blue. In all the cases the Adobe Photoshop (Adobe, San Jose, CA, USA) software was used for the post-production of images.

UVF images were captured by means of a Xnite Nikon D810 camera (Nikon Corporation, Tokyo, Japan) coupled with a PECA 916 digital filter (Peca Products Inc., Beloit, WI, USA). The illumination was obtained by means of two UV Labino<sup>®</sup> spot lamps UV light MPXL and UV FLOODLIGHT (Labino, Stockholm, Sweden) with emission peak at 365 nm. A white standard Spectralon<sup>®</sup> (Labsphere Inc., NH, USA, nominal reflectance: 99% in the field of imaging) was used for the white balance.

To carry out IRR images, the sculpture was illuminated by means of two 800W Varibeam halogen lamps (Ianiro, Eagle Beaming International Co. Ltd., New Taipei City, Taiwan) and photographed by means of the Xnite Nikon D810 camera equipped with an infrared filter (R72, Hoya, HOYA CORPORATION, Tokyo, Japan) for detecting the wavelengths in the range 780–950 nm. In this case a ColorChecker<sup>®</sup> Classic 24 colours (X-Rite, MI 49512, Grand Rapids, MI, USA) placed in the field of imaging was considered for the chromatic balance.

VIL images were acquired using the same Xnite Nikon D810 (digital camera but equipped with a Peca 910 filter (Peca Products Inc., Beloit, WI, USA, 750–950 nm). The illumination was obtained by means of a LED light with 400–700 nm emission and a Peca 916 filter placed on it. As references, both a ColorChecker<sup>®</sup> Classic 24 colours and a pad of Egyptian blue (Kremer Pigment n° 10060) were used.

To better understand the composition of painting materials and to contribute in confirming the relevance of the surface layer to the original materials, micro-invasive analysis were performed on micro-samples. Samplings were made in significant areas of the sculpture. In particular, for the stratigraphic study small pieces were taken from the body (layers sequence is shown in Figure 2a) and from the wig (layers sequence is shown in Figure 2b). Moreover, a small amount of powder was extracted from the white belt and from the brown paint covering all the surface of the sculpture. To minimize the invasiveness, no samplings were made on yellow decorations, on the black lines on the wig and on the basement because they were considered not significant for conservation aims.

The samples from body and wig were prepared in a polished section and were observed by means of a BX51 mineropetrographic microscope (Olympus Corporation, Shinjuku, Tokyo, Japan) in visible and UV light, interfaced to a PC by means of a digital camera. The acquisition and processing of images is carried out using the proprietary software analysis Five.

SEM-EDX measurements were performed in order to determine the chemical composition of the main minerals. A JSM-IT300LV scanning electron microscope (JEOL, Tokyo, Japan) equipped with an energy-dispersive X-ray spectrometer (EDX), with a SDD (Oxford Instruments, Oxford, UK), hosted at the Earth Science Department of the University of

Torino, was used for the determination of major elements. The measurements were conducted in high vacuum conditions after covering of the sample surface with a conductive layer. Spot analyses were acquired under the following conditions: accelerating voltage 15 kV, counting time 50 s, process time 5  $\mu$ s and working distance 10 mm. The EDX-acquired spectra were corrected and calibrated both in energy and in intensity thanks to measurements performed on cobalt standard introduced in the vacuum chamber with the samples. The Microanalysis Suite Oxford INCA Energy 200 (Oxford Instruments, Abingdon, Oxfordshire, UK) that enables spectra visualization and elements recognition, was employed. A ZAF data reduction program was used for spectra quantification. The resulting full quantitative analysis was obtained from the spectra, using natural oxides and silicates from Astimex Scientific Limited® (Astimex, Kista, Sweden) as standards. All the analyses were recalculated using the MINSORT computer software [16].

Preliminary ion beam analyses (IBA) measurements, in particular micro-particle induced X-ray emission (PIXE) tests were carried out in order to determine the presence of minor and trace elements in correlation with each pigment layer. This information could be useful to characterize the material and to find markers helpful in identifying different productions in time. IBA measurements were carried out at the micro-beam line of the Legnaro National Laboratory (INFN-LNL) located in Padova (Italy), using a 2 MeV proton beam. Because samples are placed in a vacuum chamber for the measurements, they were prepared following a procedure reported elsewhere [17], which is similar to the one used for SEM analysis.

Fourier transform infrared (FT-IR) spectroscopy was carried out to characterize the white pigment of the belt and brown surficial layer. The measurements were conducted on selective micro-samples with a Vertex 70 FT-IR spectrophotometer (Bruker, Billerica, MA, USA) coupled with a Bruker Hyperion infrared microscope working in transmission mode with the aid of a diamond cell.

On a sample from the brown layer, pyrolysis-gas chromatography/mass spectrometry (Py-GC/MS) was performed with an EGA/PY-3030D pyrolyzer (Frontier Lab, Koriyama, Fukushima, Japan) interfaced with a 6890N Network GC System (Agilent Technologies, Wilmington, DE, USA) with HP-5 cross-linked 5% Ph Me silicane capillary column (30 m  $\times$  0.25 mm  $\times$  0.25  $\mu$ m) and a 5973 Network Mass Selective Detector (Agilent Technologies). The sample was derivatized with the thermally assisted hydrolysis and methylation (THM) method using tetramethylammonium hydroxide (TMAH) in aqueous solution at a concentration of 25% by weight (Sigma-Aldrich, Milan, Italy). Pyrolysis was carried out at 650  $^{\circ}$ C for 12 s. The interface temperature of the pyrolyzer and of the injector of the gas chromatograph was 300  $^{\circ}$ C. The following temperature program was used for the gas chromatographic separation: isotherm of 2 min at 50  $^{\circ}$ C, ramp of 10  $^{\circ}$ C/min up to 300  $^{\circ}$ C, isotherm at 300  $^{\circ}$ C for 5 min. The carrier gas was helium (1.0 mL/min) and split ratio was 1/20 of the total flow. Mass spectra were recorded under electron impact at 70 eV, scan range 40–650 m/z. The interface was kept at 280  $^{\circ}$ C, ion source at 230  $^{\circ}$ C and quadrupole mass analyzer at 150  $^{\circ}$ C. All instruments were controlled by Enhanced Chem Station (ver. 9.00.00.38) software. The mass spectra assignment was done with the Wiley 138 and NIST2008 libraries and by comparison with literature data.

## 2.2. Mockups for Cleaning Test

### 2.2.1. Mockups

On the basis of the results on pigment characterization (described in Section 3.1), seven different layers of colours have been prepared on glass slides, in five replicas (series). A picture of the samples as prepared is shown in Figure 4a. Due to the presence of losses and superficial abrasions, experimental preliminary activity to define the better cleaning treatment was carried out on mockups featuring also the paints underneath the brown top layer (samples A–D in Figure 4a). Samples E, F and G, which mimic the polychromies underneath the brown top layer, have been used to test the effect of different cleaning procedures on surfaces with variable roughness underneath the brown layer. Commercial

products were used to prepare the mockups, even if we are aware of the unlikelihood of a real replicability of the original materials, with particular reference to proper production processes and aging. Concerning the reproduction of the brown layer, due to its complexity and in consideration of the main aims of the experimental activity, a mixture of earth pigments chromatically comparable to the original brown was considered adequate. For all the samples, extra quality gum Arabic (Bresciani Srl, Milan, Italy) at 10% in water and micronized calcium carbonate (CTS Europe, Milan, Italy) were used as a binder for paint layers and for preparation layer, respectively. Mockups' composition is summarized in Table 1.

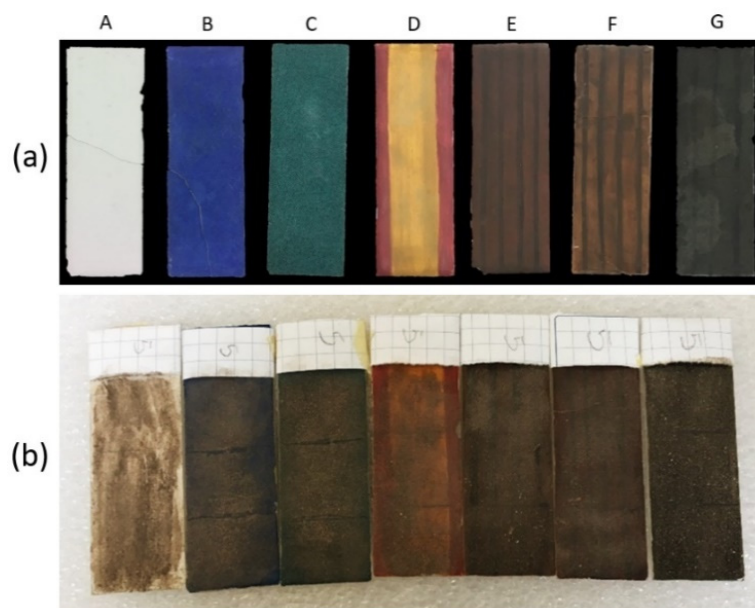


**Figure 4.** Mockups (series 5) used for cleaning trials, before (a) and after the soiling procedure (b). In the soiled samples, the reference area is covered with a white paper tissue.

**Table 1.** Mockups' composition. Preparation layer is calcium carbonate with gum Arabic as binder (10% solution in water), Brown is a mixture of 50% Burnt umber (Z.C0798), 25% Red ochre (Z.C0008) and 25% Green earth (Z.C0320).

Model Sample	Pigments of Paint Layer <sup>1</sup>	Layering of Materials <sup>1</sup>
A	None	Preparation layer
B	Egyptian blue (KP.10060)	Preparation layer-KP.10060
C	Egyptian green (KP.10064)	Preparation layer-KP.10064
D	Yellow ochre (KP.40301) + Red ochre (Z.C0008)	Preparation layer-KP.40301-Z.C0008
E	Yellow ochre (KP.40301) + Black (S.7060030) + Brown	Preparation layer-KP.40301-S.7060030 (lines)-Brown
F	Red ochre (Z.C0008) + Black (S.7060030) + Brown	Preparation layer-Z.C0008-S.7060030 (stripes)-Brown
G	Egyptian green (KP.10064) + Black (S.7060030) + Brown	Preparation layer-KP.10064-S.7060030 (lines)-Brown

<sup>1</sup> Pigment manufacturers: KP = Kremer Pigment; Z = Zecchi; S = Sinopia.

A first step of artificial ageing has been foreseen to simulate the oxidation and degradation of the binders. The samples have been aged for 500 h in a simulating solar irradiation solar box Heraeus Suntest CPS (Heraeus Holding GmbH, Hanau, Germany) equipped with a filtered (coated quartz glass simulating a 3 mm window glass, cutting  $\lambda < 300$  nm) xenon lamp and with an average irradiation of  $750 \text{ W/m}^2$  and an internal temperature of about  $50 \text{ }^\circ\text{C}$ .

After the first step of ageing, we simulated the fatty superficial dirt detected on the artefact (Figure 4b), by applying a thin layer of INCI hands cream (Yves Rocher<sup>®</sup>, now Rocher Group<sup>®</sup>, Rennes, France) to obtain a greasy surface capable of incorporating dust.

Dust was recovered from the filter of a museum vacuum cleaner commonly used in maintenance operations by Centro Conservazione e Restauro La Venaria Reale professionals. On each sample, a small area was covered during the application to be used as a reference. After applying a thick coat of dust, samples were placed in a humidity non-watertight craft chamber, realized with a wooden structure covered with Melinex® foils. Water at 25 °C was nebulized until saturation, and samples were left there for 4 h, i.e., the time needed to return to the outside environmental conditions. This procedure allowed dust to better adhere to the surfaces. Afterwards, dust excess not firmly attached to the surface was removed shaking the mockups upside down and using a compressed air jet by means of an airbrush.

### 2.2.2. Selected Cleaning Materials

Latex free high-density polyurethane (PU) sponges (Deffner&Johann®, Röthlein, Germany) have been compared with innovative highly retentive hydrogels. The use of this specific PU sponges is common in the professional practice in case of archaeological materials, with procedures that follow the results of a European research project specifically dedicated to dry-cleaning [8].

Among the available innovative highly retentive hydrogels recently introduced in conservation practice, twin-chain polymer hydrogels based on poly(vinyl alcohol), developed within the H2020 European project NANORESTART (grant agreement 646063), were selected. One of the most interesting features of these systems is their capability of adapting to the three-dimensional objects and irregular surfaces, such as the painted areas of the Egyptian sculpture. Moreover, the hydrophilic poly(vinyl alcohol)-based structural network makes the gel capable of holding large amounts of aqueous liquid, while the highly retentive properties limit the liquid's penetration so that cleaning occurs only at the interface, without affecting the surrounding area or leaving residues. Within the European project, formulations were tailored to adapt to the specific requirements of several case studies, but also served as prototypes for a series of multipurpose gels, which were formulated to target typical cleaning cases. Gels are named Nanorestore Gels® Peggy 5 and Nanorestore Gels® Peggy 6 (CSGI, Florence, Italy), being the first more retentive and rigid than the second. Both formulations are available in different shapes, including thin foils (sheets) or in parallelepiped shape (gum).

After some preliminary test, Nanorestore Gel® Peggy 6 (sheets, PG6) and Nanorestore Gel® Peggy Gum 5 (PG5 Gum) were selected. The first are more flexible and easily adapt to the artefact. The second ones were selected due to their shape that provides an easier handling and allow for a gentle and punctual mechanical action, possibly increasing the efficacy of the cleaning.

With the aim of defining the best cleaning procedure, different combinations of materials and application lengths were tested, as summarized in Table 2.

**Table 2.** Cleaning tests carried out on mockups. For each sample a non-soiled area has been kept as reference.

Materials Tested on Each Sample	Objective	Test Name	Test Description
PG6	Tuning the length of gel sheet's application	2a	180 s
		2b	150 s
		2c	120 s + 60 s
		3a	90 s + 90 s
		3b	60 s + 60 s
		3c	30 s
PG6 PG5 Gum	Comparing the effect of gel gums applied on wet and dry surfaces	4a	PG6 (90 s + 90 s) + PG5 Gum on a still wet surface
		4b	PG6 (90 s + 90 s) + PG5 Gum on a dried surface
PG6 PG5 Gum PU sponge (DJ) <sup>1</sup>	Comparing the best result obtained with hydrogels with the traditional dry cleaning method	1a	PG6 (90 s + 90 s) + PG5 Gum on a dried surface
		1b	Mechanical removal. Sponges previously washed in demineralized water
PG6 PG5 Gum PU sponge (DJ) <sup>1</sup>	Evaluating the boost in efficacy by combining the two methods	5a	PU sponge (DJ) <sup>1</sup> + PG6 (90 s) + PG5 Gum on a dried surface
		5b	PU sponge (DJ) <sup>1</sup> + PG6 (120 s)
		5c	PU sponge (DJ) <sup>1</sup> + PG5 Gum on a dried surface

<sup>1</sup> DJ = Deffner & Johann®



### 2.2.3. Assessment of Cleaning Results

Colorimetric analyses were used to assess the efficacy of the cleaning methods in terms of removal of the dirt layer. Three replicas for each measurement were acquired. A Konica Minolta CM-700d colorimeter (Konica Minolta, Osijek, Croatia), with a range of measurement of 400–700 nm, step 10 nm, measurement field of 3–8 mm, d/8 geometry, standard D65 illumination and standard 10° observer was used. The measures were expressed in L\*, a\* and b\* colour space coordinates CIE 1976 and in cylindrical space CIELCH. The specular component included (SCI) data, which allows obtaining results closer to the human eye sensitivity to colours was used.  $\Delta E$  was calculated using the  $\Delta E_{00}$ , starting from the colorimetric coordinates of samples before soiling and after cleaning operations [18].

Optical microscopy was used on sponges and gels after use, to verify the presence of grains of pigment and thus to evaluate the invasiveness of each test method. Besides this, optical microscopy was carried out to monitor the effects of treatments on the surfaces before and after treatments. The equipment used in this phase was an OLYMPUS SZ X10 (Olympus Corporation, Shinjuku, Tokyo, Japan), interfaced with a PC through a digital camera OLYMPUS Color View I. For capturing and processing the images, analySIS Five software was used.

In addition to this, we documented eventual changes in morphology of the surface, by reflectance transformation imaging (RTI) both before soiling and after the treatments. The RTI technique, based on computational photography, enables the interactive relighting of a subject from any direction, and it is normally used on small areas to emphasize tiny aspects of the surface [19,20]. The samples selected were the ones with the calcite layer only, which are more sensitive to water-based treatments, and with Egyptian Blue and Green ones, for their grain size (respectively the type A, B and C).

Referring to the preliminary measures acquired on the case study, necessary to better calibrate the conservation treatments, we carried out conductivity and superficial pH measurements; the first one has been acquired to work in isotonic conditions with the original painted surface and the second to avoid ionizing action of the cleaning solution [21]. A 2 mm thick pad of agarose (4% in demineralized water) was applied on the object surface for 120 s after having removed the main layer of dust. Conductivity measurement was performed with a LAQUAtwin conductivity meter EC-22 range (Horiba, Kyoto, Japan) and pH analysis was performed with a Hanna Instrument HI 981037 Skin and Scalp pH Tester (Hanna Instruments, Woonsocket, RI, USA).

## 3. Results and Discussion

### 3.1. Painting Materials Characterization

Figure 5 shows the OM images of the two sections sampled from the wig (Figure 5a, sample A) and from the body (Figure 5b,c sample B) of the sculpture. The main painting layer scheme described in Figure 2 is visible. In particular, from the bottom to the top of the wig sample a green-white-red-brown sequence is clearly distinguishable (Figures 5a and S1). In this case the first white preparation layer is not recognizable because it was not included in the sampling procedure. Regarding the sample from the body (Figure 5b with a detail in Figure 5c) the first white preparation layer can be seen in the bottom part of the stratigraphy. In this case the sequence is white-blue-white-green-brown. The brown layer seems to be thicker in the body compared to the wig. By means of VIL, SEM-EDX, FTIR, Py-GC/MS and FT-IR all the principal painting layers observed in OM images were identified. Micro-PIXE was used to obtain additional information on minor and trace elements.

FTIR and micro-PIXE spectral data as well as the SEM-EDX results (elemental analysis) are provided as Supplementary Material.

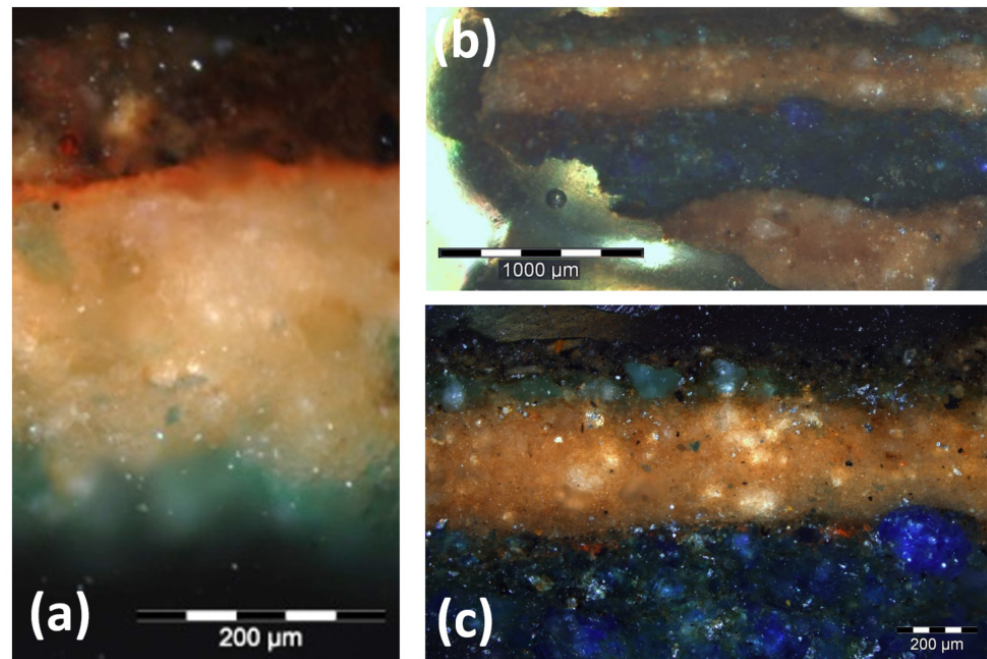


**Figure 5.** Optical Microscopy images (OM) of the two samples taken from the wig (a), sample A, and the body (b,c), sample B, of the sculpture; (c) is a magnification of a portion of sample B.

### 3.1.1. Blue and Green Pigments

For what concerns the blue pigment, the preliminary analysis by means of VIL was useful to identify it as Egyptian blue. In Figure 6b a relevant image of VIL compared with photograph is shown. The luminescence was observed only in the body part of the sculpture and not in the head. VIL results were confirmed by means of SEM-EDX on the sample B where a thick blue layer is present. The stoichiometry obtained from homogeneous blue crystals by means of SEM-EDX (Figure S2) is very close to that of cuprorivaite ( $\text{CaCuSi}_4\text{O}_{10}$ ). In the blue layer, a significant amount of quartz, partially bonded together with a glass, is present, coherent with available literature [22].



**Figure 6.** Photographs of part of legs (a) and of back/wig; (c) VIL image of the same part of the legs (b) in which the luminescent areas are made of Egyptian blue; (d) IRFC image of the back/wig in which green pigment (turquoise color) is more evident.

The green pigment was observed both in the wig as the first layer over the white preparation layer, and as a final layer under the brown uppermost layer in the body. In Figure 6d the IRFC image of part of the back and wig shows a turquoise tone where the thin green layer is located. Instead, in the same picture, the Egyptian blue shows a red tone. By means of SEM-EDX analysis it was possible to confirm that the pigment is Egyptian Green or green frit. The use of Egyptian Green in antiquity seems to be confined to Egyptian territory, with first evidence in the last part of the third millennium BCE [23]. In terms of microstructure, the green frit consists of glass, from which wollastonite ( $\text{CaSiO}_3$ ) and a high temperature polymorph of silica have crystallized, together with partially reacted quartz particles [22]. In Figure 7 is shown a SEM-BS image of a green crystal observed in sample B in which the two-phase microstructure is clear. In particular, by means of SEM-EDX (Figure S3) it was detected that the light grey part of the crystal is made of wollastonite with the addition of sodium and copper, whereas the dark grey part is a silica-rich amorphous phase with calcium, sodium and copper. In average, in the two samples, the green portion has a lower copper content and a higher sodium content than blue portion. These differences are imputable to the different production processes as described by [22,24]. Preliminary results by means of micro-PIXE (Figure S4) have shown some differences in trace elements composition, in particular in potassium content, for the green sectors from sample A and sample B (i.e., the green pigment that form the first buried layer in the wig and the green pigment below the brown layer in the body), even though counting statistic is low and further analyses are necessary to confirm the observation and to correlate it to the chronology of the layer sequence.

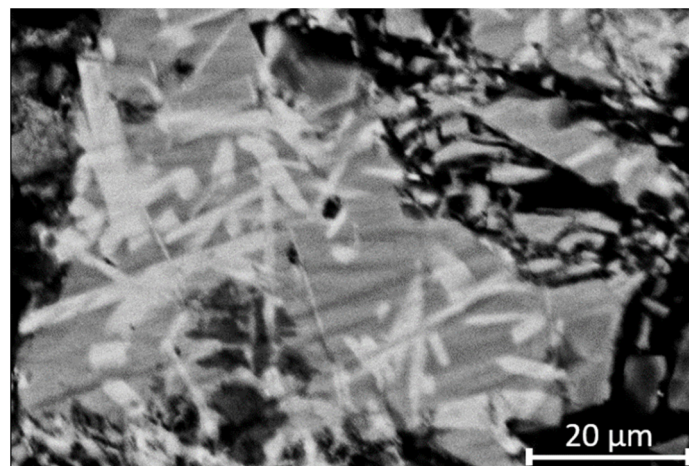


**Figure 7.** SEM-BS image of a green portion observed in sample B where it is possible to observe two-phase system (light gray is wollastonite, dark gray is high temperature polymorphs of silica).

### 3.1.2. The brown Pigment Layer

For what concerns the development of a suitable cleaning procedure, the last layer, i.e., the surface brown pigment, is indeed the most important to be studied (Figure 8). This layer covered most of the polychromies of the sculpture, raising a question about its removal. In that sense, the evaluation of its pertinence to the original artistic technique would have been fundamental to consider its eventual removal. Analyses have shown that it is composed by an organic material in which are included many different mineral crystals. FTIR analysis was not able to distinguish any features due to the strong presence of oxalates.

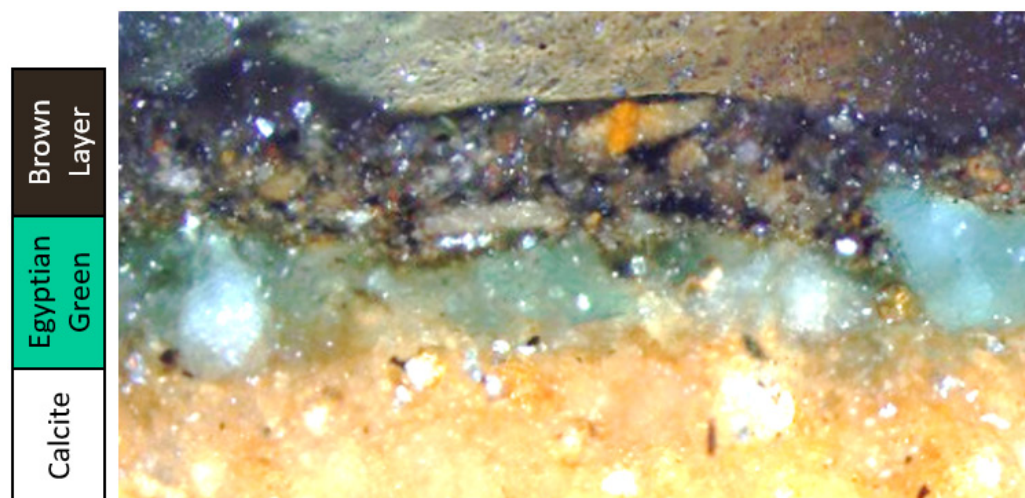


**Figure 8.** OM images of a details of the stratigraphy of sample B in which is highlighted the complexity of the brown layer over the Egyptian green.

In order to understand the nature of the organic components of the brown material, a pyrolysis-gas chromatography/mass spectrometry analysis was carried out, derivatizing the sample with TMAH. The analysis of the pyrogram allowed to identify a series of marker compounds of substances compatible with materials of natural origin used in ancient Egypt, while no organic materials of synthetic origin were identified. Table 3 contains the list of all peaks for which it was possible to make a certain assignment. Minimal traces of protein markers were also identified, not indicated in the table as they are not significant to clarify the nature of the sample. The Py-GC/MS curve is shown in Figure 9.

**Table 3.** Marker compounds of organic materials identified by Py-GC/MS in the brown surface layer of the sculpture.

Peak n.	Retention Time [min]	Assignment
1	5.95	1,2,3-Trimethoxypropane
2	8.08	2-Butendioic acid dimethyl ester
3	8.27	2-Butendioic acid dimethyl ester
4	9.32	Benzoic acid methyl ester
5	11.71	2-Methoxybutendioic acid dimethyl ester
6	12.15	Permethylated 3-deoxypentenoic acid methyl ester
7	12.40	Permethylated 3-deoxypentenoic acid methyl ester
8	13.16	Permethylated 3,6-deoxyhexenoic acid methyl ester
9	13.32	1,2,4-Trimethoxybenzene
10	13.40	Permethylated 3,6-deoxyhexenoic acid methyl ester
11	13.42	4-Methoxybenzoic acid methyl ester
12	13.87	1,2,3-Propaentricarboxylic acid trimethyl ester
13	14.25	Octanedioic acid dimethyl ester
14	14.69	Permethylated 3-deoxyhexenoic acid methyl ester
15	15.17	Permethylated 3-deoxyhexenoic acid methyl ester
16	15.49	Nonanedioic acid dimethyl ester
17	16.08	3,4-Dimethoxybenzoic acid methyl ester
18	16.39	2,3,4,6-Tetra-O-methyl-D-gluconic acid $\delta$ -lactone
19	17.51	Tetradecanoic acid methyl ester
20	17.56	3,4,5-Trimethoxybenzoic acid methyl ester
21	18.67	1,2,3-Benzentricarboxylic acid trimethyl ester
22	18.86	1,2,4-Benzentricarboxylic acid trimethyl ester
23	19.39	9-Hexadecenoic acid methyl ester
24	19.62	Hexadecanoic acid methyl ester

Table 3. Cont.

Peak n.	Retention Time [min]	Assignment
25	21.30	9-Octadecenoic acid methyl ester
26	21.54	Octadecanoic acid methyl ester
27	23.27	Eicosanoic acid methyl ester
28	24.89	Docosanoic acid methyl ester
29	25.65	21-Methyldocosanoic acid methyl ester
30	26.15	Heptacosane
31	26.40	Tetracosanoic acid methyl ester
32	26.86	Octacosane
33	27.09	Squalene
34	27.59	Nonacosane
35	27.86	Hexacosanoic acid methyl ester
36	28.38	Tricontane
37	29.36	3-Methoxycholest-5-ene
38	29.65	Octacosanoic acid methyl ester

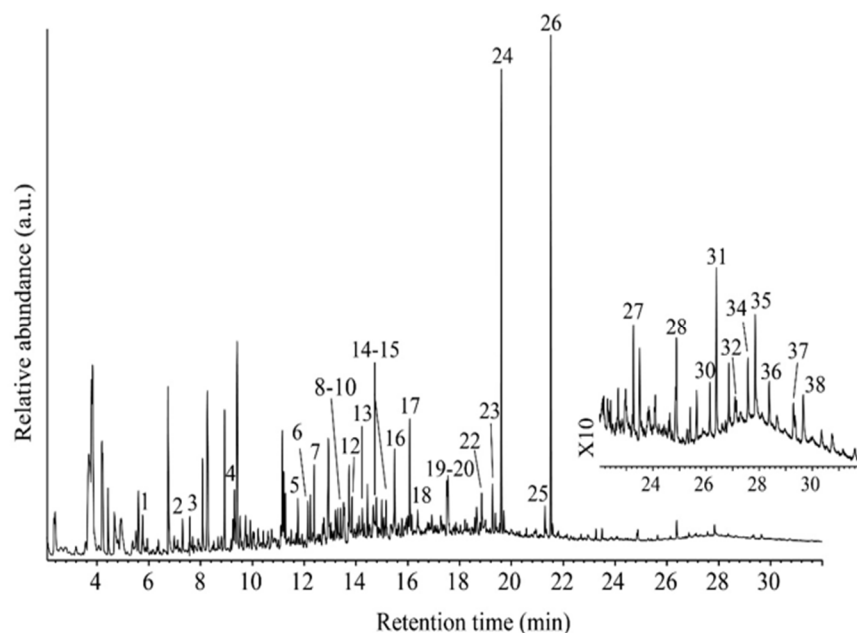


Figure 9. Pyrogram of the surface paint layer of the sculpture. For assignments see Table 3.

The two most intense signals are attributed to palmitic (peak n. 24) and stearic acid (n. 26), detected in the form of methyl esters. Longer chain saturated fatty acids have also been identified, with a number of carbon atoms from  $C_{20}$  to  $C_{28}$  (n. 27, 28, 29, 31, 35, 38), and some unsaturated fatty acids (n. 23, 25). These compounds, together with  $C_{27}$ – $C_{30}$  linear alkanes (n. 30, 32, 34, 36), are markers of lipidic substances such as natural waxes. However, the specific markers of the main natural waxes (e.g., 15-hydroxyhexadecanoic acid for beeswax) are missing. The presence of cholesterol (n. 37) could be due to the use of an animal wax or animal fats, not better identified and probably mixed with other fatty substances [25,26]. These same compounds are also present in human sebum and could be due to the manipulation of the object, a hypothesis also supported by the presence of squalene, a marker compound present in fingermarks [27]. Moreover, the peaks assigned to glycerol (n. 1) and dicarboxylic acids with eight and nine carbon atoms (here detected as dimethyl esters, n. 13 and 16) can be related to glycerol-based lipids of oils, fats or body lipids of microorganism that might be present in the sample.

The other compounds identified by Py-GC/MS belong to two different chemical classes, saccharides and aromatic compounds such as phenols and hydroxyaromatic acids.

As for saccharides, markers derived from arabinose (n. 6, 7), rhamnose (n. 8, 10) and galactose (n. 14, 15) have been detected, as expected for gum Arabic [28]. Gum Arabic was extensively used as binding medium in ancient Egypt, therefore its finding on the surface of the sculpture is consistent with the presence of a paint layer [23,29]. Furthermore, yellowing of gum Arabic due to aging has been associated with the darkening of paints containing Egyptian blue, which in many ancient artefacts appear brownish green or almost black [30]. This phenomenon, observed on several objects decorated with Egyptian blue paints, could be co-responsible for the current visual aspect of the sculpture.

Some of the aromatic compounds identified (n. 17, 20) could be attributed to a contamination due to the wood material of the sculpture [31]. However, the building-block compounds of lignin (i.e., methyl, ethyl, *n*-propyl and vinyl guaiacols) are absent, so it appears more likely that their origin is different. The same compounds were identified in Egyptian mummification balms and it was hypothesized that they are oxidation products of balsamic resins secreted by plants of the Umbelliferae family [32]. Hydroxyaromatic acids are also markers of humic acids and tannin-derived materials (n. 2, 3, 4, 5, 9, 11, 17, 20) [33,34]. The latter are particularly interesting because of their brown colour which tends to black when combined with iron [35]. These compounds could also contribute to the dark colour of the superficial layer of the sculpture.

To investigate in deep the brown layer, a petrographic study of the mineral grains included in the gum was carried out to verify its compatibility with an Egyptian territory origin. In particular, a fine sand formed by clasts smaller than 100 microns is present (Figure 10).

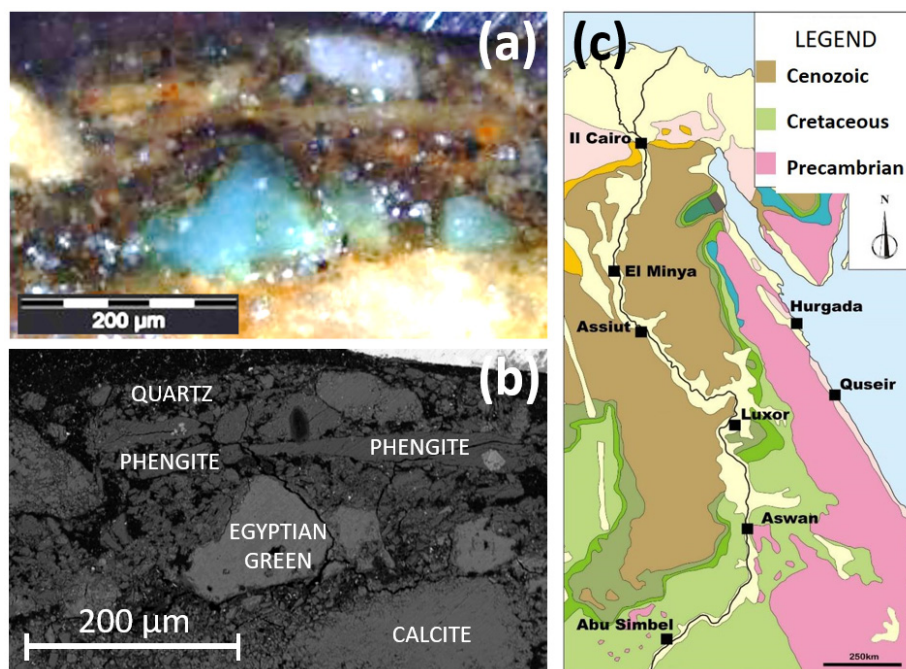


**Figure 10.** OM (a) and SEM-BS (b) images of the surface layer that is composed by an organic material in which different minerals are dispersed; simplified geological map of Egypt (c).

Numerous mineral particles were observed in this layer consisting mainly of quartz, calcite and white mica. In accessory quantities there are also biotite, pyroxene, iron oxides, apatite and sulphides. Respect to the provenance study, among the various minerals found, the most interesting was potassium white mica. It constantly shows a phengitic composition, in the sense that it shows an enrichment in Si and a reduction in Al, compared to the theoretical formula of muscovite [36]. In the literature, phengite is commonly associated with metamorphic rocks that formed under conditions of high pressure, in the subduction zones [37]. This therefore allows to confirm the compatibility with Egyptian

territory and to constrain the area of origin of the raw material used by the Ancient Egyptians, as part of the covering layer of the statue in question. By observing a simplified geological map of Egypt, the territory can be divided into three main geological units (see Figure 10c). In the central-northern sector of Egypt, sedimentary rocks of carbonate origin from the Cenozoic age mainly crop out [38]. The presence of abundant silicate clasts in the analysed sample makes it possible to exclude with good approximation that the material used comes from this sector of Egypt and, in particular, from the delta area of the Nile. In the southern sector of Egypt, on the other hand, sedimentary rocks of the Cretaceous age referred to the Nubian Sandstone Formation occur [39]. Even the outcrop area of these sandstones can be excluded as the area of origin of the raw material, as the Nubian sandstones are extremely pure and almost exclusively made up of quartz clasts. Finally, the eastern sector of Egypt is characterized by the presence of very ancient crystalline rocks (pre-Cambrian in age, corresponding over to 500 million years), which are called Arab-Nubian shield. To this geological unit belongs both the famous Aswan granites and metamorphic units of continental crust [40]. Granites very rarely contain white mica and therefore it can be excluded that the material comes from the Aswan area. Instead, the different metamorphic units out cropping in the Egyptian Eastern Desert are characterized by metamorphic conditions favourable to the stability of phengitic mica. In particular, the eastern desert is crossed by the Wadi Hammamat, an ancient road link between the Nile and the Red Sea, frequented by the Ancient Egyptians since the fourth dynasty and especially in the Ramesseid era, a period to which the production of the Papyrus of the Mines also dates back [41]. Therefore, based on the mineralogical data collected using the SEM analysis, it is possible to infer that the raw material for the covering layer of the sculpture is compatible with Egyptian territory. Probably it comes from areas of the eastern desert and was transported along the Wadi Hammamat, while other sources such as the Nile delta and the Aswan area are to be excluded.

### 3.1.3. Other Pigments

The red pigment in the sample A (taken from the wig) was attributed to red ochre because from SEM-EDX analysis it turns out to be rich in iron with minor contents of other elements such as silicon, aluminium, magnesium and potassium (Figure S1). The result was confirmed also by means of micro-PIXE measurements. Red ochre was a very common pigment used starting from the fourth millennium BCE through the Roman period [23].

All the white layers used as preparation, both in sample A and sample B, are made of calcite, another very common material employed in Ancient Egypt starting from the Predynastic Period [23]. No presence of sulphur as main element was observed, excluding the use of gypsum or anhydrite. Moreover, from preliminary micro-PIXE (Figure S4) analysis no particular differences were observed in minor and trace elements (Si, S, Cl, Fe and Cu) in the intermediate and first layers, even though the result is not sufficient to hypothesize a contemporaneity of the two layers.

For what concerns the decorative elements, FT-IR analysis (Figure S5) carried out on a sample from the white belt have shown the presence of huntite,  $Mg_3Ca(CO_3)_4$ , a carbonate mineral which provides a brighter white than calcite. Its use in Ancient Egypt is documented starting from third millennium BCE [23].

No analyses were considered necessary to understand the artwork for conservation purposes on black and yellow decorations. The black pigment is made probably of charcoal or carbon also considering their strong absorption in IR images, and the yellow pigment was attributed to yellow ochre, in consideration of literature, its hue and morphology [42].

### 3.2. Cleaning Tests on Mockups

Following the conservation cleaning treatments guidelines, preliminary tests were carried out on mockups (see Table 1) to evaluate the effect of each selected method with the aim of defining the safest and most efficient cleaning protocol to treat the original surface.

The first cleaning tests were performed using the two selected cleaning methods alone, i.e., PU sponges and highly retentive hydrogels. In particular, we focused in finding the best combination of application length and number of applications for PG6. Then, we evaluate the effectiveness of PG5 Gum to finalize a cleaning procedure performed with PG6. Results obtained using the two cleaning methods alone were then evaluated. Afterwards, in order to take advantage of the strengths of the tested methods and to minimize their weaknesses, we combined the dry and the water-based cleaning treatments. The characterization of samples before and after cleaning tests allowed to evaluate the performances of the materials and to determine the failure point of each treatment.

Several tests were carried out using PG6 to define a time range to work safely and efficiently on the surface to be cleaned, i.e., the maximum and minimum length of application were defined. Thanks to the OM, we observed that after the application of a PG6 for 180 s, a partial alteration of the substrate took place, as testified either by the presence of bigger grains on the gel's surface in contact with the substrate to be cleaned or by colour changes in the applied gel. On the other hand, applications shorter than 90 s did not result an effective cleaning of the surface.

Moreover, we compared the effect of a single long application with two subsequent shorter applications, having the same or higher overall contact time. For instance, we noticed that a single 2-min-long application allowed to obtain good cleaning results but caused a partial migration of the pigment from the surface. On the other hand, a two steps application provided comparable results, without changes in the original materials, granting higher control on the cleaning action. Overall, the most promising results were obtained with a two-step application of PG6 (3a test, 90 s + 90 s), although some residues of dirt were still present on the surface, requiring a localized refining of the cleaning.

To that aim, PG5 Gums were tested both on dry (after complete evaporation of the water released by PG6) and wet (immediately after the application of PG6) surfaces. PG5 Gums performed in a satisfying way for the localized removal of dirt residues. It is worth noting that, during application, the gum should be gently handled (not squeezed) to prevent uncontrolled release of water. Overall, the best results were obtained by the application of PG5 Gum over the dry surface, which withstands a mechanical action, even if gentle, better than wet and softened materials.

The single methods (PU sponges and the best PG systems combination) showed a good potential for the cleaning of water-sensitive surfaces, even if both displayed some limitations. In particular, PU sponges efficiently removed the dust layer, but at the expense of the integrity of the original paint layer. In fact, several coloured particles were detected on the surface of the sponges, especially when applied on mockups prepared using pigments with larger grains (see Figure 11a). On the contrary, highly retentive hydrogels did not interfere with the original material, i.e., no coloured particles were detected on gel's surfaces (see Figure 11b), but the system only partially removed the dirt layer, providing an incomplete cleaning effect.

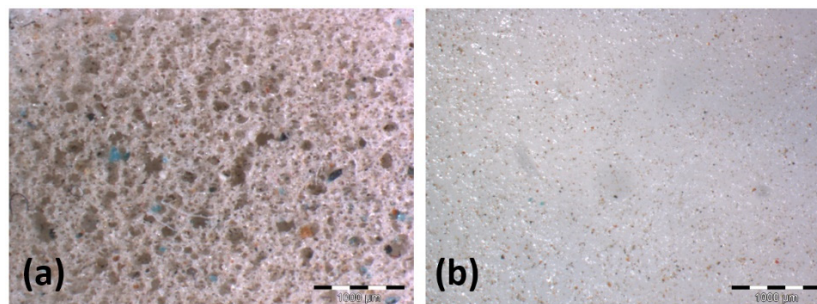


**Figure 11.** (a) OM image (25 $\times$ ) of the PU sponge after cleaning at the interface of green sample (set n.1); (b) OM image (25 $\times$ ) of the PG6 after cleaning at the interface of blue sample (set n.2).



For this reason, as indicated in Table 2, we tested different combination of the two methods, to define an effective cleaning procedure (tests' series 5). The best results were obtained with a preliminary gentle dry-cleaning step that provided a partial removal of the dirt without altering the original surface. The second step, carried out with PG6 (90 s) removed the dirt layer left on the surface without damaging the treated material. PG5 was then applied on dried samples, refining the cleaning with a localized action completely respectful of the original material (5a set, Figure 12).



**Figure 12.** 5a set after cleaning tests using best conditions. Not soiled area on the top.

To confirm the optical evaluation and the OM results, colorimetric measurements were carried out on this set of samples before soiling and after cleaning. The obtained  $\Delta E_{00}$  span between a maximum of 8.9 and a minimum of 1.3, with higher values corresponding to samples B and C (Egyptian Blue and Green without the top brown layer), because of their superficial roughness, which hampered a homogenous cleaning, and lower values measured on samples A and F (preparation layer only and ochre with yellow stripes). Nevertheless, considering the complexity of the prepared samples, the colorimetric changes measured were deemed acceptable and the overall cleaning results were considered satisfactory. Moreover, RTI analysis did not detect any significant morphological change on the surface after the combined application of PU sponges or the innovative hydrogels (Figure 13), confirming the safeness of the used cleaning procedure.

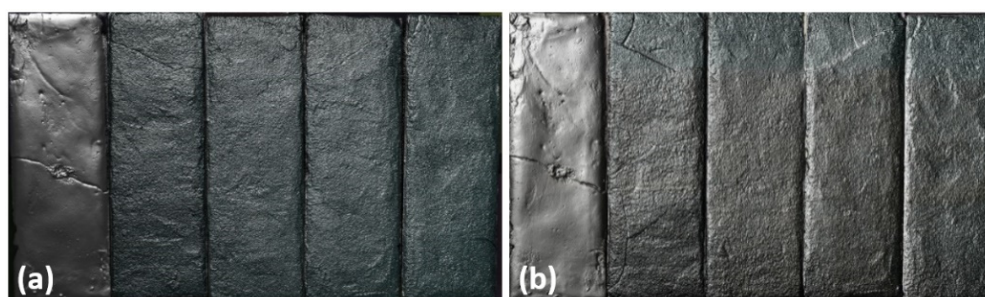


**Figure 13.** RTI documentation before (a) and after (b) cleaning tests.

### 3.3. Cleaning Treatment of the Egyptian Statuette

A careful analysis of the pictorial surface revealed problems of stability for the entire stratigraphy, which showed a loss in the adhesion at multiple stratigraphic levels often combined with partial detachments of the material at the underlying interface. Moreover, due to the loss of cohesion of the Egyptian Blue layer belonging to the first pictorial level, the sculpture showed several cracks within this layer, with a consequent embrittlement of the entire stratigraphy. Therefore, it was decided to consolidate the pictorial layers before

the cleaning treatment, by injecting locally, only where needed, a solution of hydroxyl propyl cellulose (Klucel G<sup>®</sup>, CTS Europe<sup>®</sup>, Milan, Italy, 2% in ethanol), which was deemed compatible with the original materials.

After that, based on the results obtained on mockups, we selected the best procedure for the superficial cleaning of the Egyptian statuette. The measure of pH (6.62) and conductivity (3  $\mu\text{S}/\text{cm}$ ) suggested not to consider necessary to use a buffer solution, so as to avoid any need of rinsing the surface with a subsequent application of water-loaded gels to remove buffer residues.

The tests conducted on mockups were fundamental for the cleaning of the artefact. However, as expected, some adjustments have been performed during cleaning operations, especially where a thicker layer of dirt was present. In those areas, a 2-min-long single application of PG6 was needed to remove most of the soil. The finishing of the cleaning was carried out with PG5 Gum, which were deemed particularly useful in areas with major undercuts.

Overall, the selected cleaning procedure of the artefact increased the perception of the painted decoration, leading to a general matting of the surface that results in a clearer tone of the brown layer, according to its supposed original appearance (Figure 14).



**Figure 14.** The artefact after the cleaning treatments.

#### 4. Conclusions

The characterization of the original materials collected from the surface of the statue confirmed the use of a colours' palette typical of the Ancient Egyptian production and a complex layering of the polychromies. For what concerns the white pigment, calcite was used for the preparation layers and huntite for the belt decoration. Red ochre was employed for the wig and probably for the base of the sculpture. Moreover, Egyptian Blue was found in samples taken for the body, whereas Egyptian Green was used to colour part of the body and the wig. Interestingly, a brown pigment was used to cover the whole sculpture. Analyses have shown that it is composed by a fine sand and gum Arabic as binder. Based on the mineralogical data collected, it is possible to infer that the raw material for the

covering layer of the sculpture is compatible with Egyptian territory. Probably it comes from areas of the eastern desert, while other sources such as the Nile delta and the Aswan area are to be excluded. The dark colour of this layer might be due to several reasons: we hypothesize that the original brown colour was darkened by the alteration of the gum Arabic used as binder, and by the addition of humic acids and tannin-derived materials that could be related to the destination of use of the sculpture, possibly a funerary one.

The cleaning of ancient Egyptian artefacts is still an open problem, because it often implies the removal of overlapped materials and superficial dirt from hydrophilic, porous and extremely delicate surfaces, which often do not feature any finishing layer. For those reasons, the dry cleaning is often preferred to solvents or water-based cleaning methods. However, this specific case study had further challenges: its three-dimensionality, the fragility of the original materials, the complex layering and the irregular morphology of the surfaces complicated the cleaning process, and the chromatic similarity between the non-homogeneous dirt layer and the underlying brown pigment layer below needed an even more careful monitoring of the cleaning operations.

The application of PU sponges on mockups allowed for the almost complete removal of soil, but at the expense of the integrity of the original paint layer. In fact, several pigment grains were removed for the surface together with the dirt layer. The best results in terms of cleaning effectiveness and non-invasiveness to the original surfaces have been obtained by a gentle action using PU sponges followed by the application of highly retentive polyvinyl alcohol-based gels, namely PG6 and PG5 gums. The preliminary application of PU sponges allowed for the partial removal of the soil without altering the original surface, while the gels permitted a gradual and controlled action at the interface without removing pigments' grains. Following the promising results obtained on mockups, the ancient Egyptian statuette was cleaned successfully and safely.

To summarize, thanks to this study, we had the chance of collecting new insights about the chemical composition of the artefact, which can be fundamental for archaeologists and art historians. Moreover, it was demonstrated that, when confined in highly retentive gels, water-based systems can be safely used for the cleaning of hydrophilic surfaces. Future perspective may involve additional testing of these flexible and elastic hydrogels on other artistic surfaces that are highly reactive to aqueous-based treatments, with the aim of expanding the palette of available tools for conservators working on fragile, sensitive and delicate works of art, improving the results that can be obtained with the sole traditional dry-cleaning methodologies.

**Supplementary Materials:** The following are available online at <https://www.mdpi.com/article/10.3390/coatings11111335/s1>, Figure S1: SEM-EDX maps of the main elements in the sample A. The first image in gray scale is the SEM-BSE image, Figure S2: Elemental analysis (weight %) by means of SEM-EDX of three representative blue grains. The blue squares are the areas of analysis. On top right are shown the optical images of the grains, Figure S3: Elemental analysis (weight %) by means of SEM-EDX of a representative green grain. The green squares are the areas of analysis. In the center is shown the optical images of the grain, Figure S4: Semi-quantitative elemental analysis by means of PIXE of different green (top) and white preparation (bottom) layers, Figure S5: FT-IR analysis carried out on a sample from the white belt has shown the presence of huntite.

**Author Contributions:** Conceptualization, N.M., P.B. (Paola Buscaglia) and A.L.G.; methodology, P.B. (Paola Buscaglia) and A.L.G.; investigation, A.B., A.R., D.S., L.G., M.N., N.M., G.P. and P.B. (Piero Baglioni); data curation, P.B. (Paola Buscaglia), A.B., A.L.G., D.S., L.G., M.N., N.M.; supervision, M.B., P.G., S.A., P.B. (Paola Buscaglia) and A.L.G.; writing—original draft preparation, N.M., A.B., A.L.G., D.S., and P.B. (Paola Buscaglia); writing—review and editing, A.L.G., G.P., P.B. (Piero Baglioni) and P.B. (Paola Buscaglia); visualization, P.B. (Paola Buscaglia) and A.L.G. All authors have read and agreed to the published version of the manuscript.

**Funding:** The European Union (NANORESTART and APACHE projects, Horizon 2020 research and innovation program under grant agreement No 646063 and 814496, respectively) is gratefully acknowledged for partial financial support.

**Acknowledgments:** The authors wish to warmly thank Anna Piccirillo (Centro Conservazione e Restauro La Venaria Reale) and Tommaso Poli (Dipartimento di Chimica-Università degli Studi di Torino) for the FT-IR analyses and Daniele Demonte (Centro Conservazione e Restauro La Venaria Reale) for the multiband imaging.

**Conflicts of Interest:** The authors declare no conflict of interest.

## References

1. Baines, J. *Fecundity Figures. Egyptian Personification and the Iconology of a Genre*; Aris & Phillips Ltd.: Warminster, UK, 1985; pp. 317–318, ISBN 0-85668-087-7.
2. Mottica, R. *Scultura Ligna in Terra d’Egitto: Analisi Valutativa di una Statuetta del Dio Nilo Conservata al Museo Egizio di Torino*. Bachelor’s Thesis, Università di Torino, Torino, Italy, 2006.
3. Santoro, S. *Il Colore nell’Antico Egitto: Inquadramento e Riflessioni Tecnico-Artistiche e Simboliche sui Colori di Statuetta del dio Nilo, Integrate da Indagini Archeometriche al SEM-EDS*. Bachelor’s Thesis, Università di Torino, Torino, Italy, 2006.
4. Serrapede, M. *I Colori del Dio Nilo: Caratterizzazione delle Stesure Cromatiche di una Statuetta Ligna del Dio per Mezzo di XRF, PIXE e SEM-EDS*. Bachelor’s Thesis, Università di Torino, Torino, Italy, 2007.
5. Manfreda, N. *Conservation Problems of an Artefact with Double Layers of Polychromy: A Wooden Sculpture of New Kingdom from the Museo Egizio di Torino*. Master’s Thesis, Università di Torino in agreement with Centro Conservazione e Restauro la Venaria Reale, Torino, Italy, 2019.
6. Fabretti, A.; Rossi, F.; Lanzone, R.V. *Regio Museo di Torino. Antichità Egizie*; Stamperia Reale: Torino, Italy, 1882; Volume 1, p. 58.
7. Daudin-Schotte, M.; Bisschoff, M.; Joosten, I.; van Keulen, H.; van den Berg, K.J. Dry cleaning approaches for unvarnished paint surfaces. In *New Insights into the Cleaning of Paintings: Proceedings from the Cleaning 2010 International Conference, Universidad Politécnica de Valencia and Museum Conservation Institute*; Mecklenburg, M.F., Charola, E., Koestler, R.J., Eds.; Smithsonian Contributions to Museum Conservation; Smithsonian Institution Scholarly Press: Washington, DC, USA, 2013; pp. 209–219.
8. Baglioni, M.; Poggi, G.; Chelazzi, D.; Baglioni, P. Advanced materials in cultural heritage conservation. *Molecules* **2021**, *26*, 3967. [[CrossRef](#)]
9. Domingues, J.A.L.; Bonelli, N.; Giorgi, R.; Fratini, E.; Gorel, F.; Baglioni, P. Innovative hydrogels based on semi-interpenetrating p(HEMA)/PVP networks for the cleaning of water-sensitive cultural heritage artifacts. *Langmuir* **2013**, *29*, 2746–2755. [[CrossRef](#)] [[PubMed](#)]
10. Bonelli, N.; Montis, C.; Mirabile, A.; Bertia, D.; Baglioni, P. Restoration of paper artworks with microemulsions confined in hydrogels for safe and efficient removal of adhesive tapes. *Proc. Natl. Acad. Sci. USA* **2018**, *115*, 5932–5937. [[CrossRef](#)]
11. Cardaba, I.; Poggi, G.; Baglioni, M.; Chelazzi, D.; Maguregui, I.; Giorgi, R. Assessment of aqueous cleaning of acrylic paints using innovative cryogels. *Microchem. J.* **2020**, *152*, 104311. [[CrossRef](#)]
12. Bonelli, N.; Poggi, G.; Chelazzi, D.; Giorgi, R.; Baglioni, P. Poly(vinyl alcohol)/poly(vinyl pyrrolidone) hydrogels for the cleaning of art. *J. Colloid Interface Sci.* **2019**, *536*, 339–348. [[CrossRef](#)] [[PubMed](#)]
13. Bartoletti, A.; Barker, R.; Chelazzi, D.; Bonelli, N.; Baglioni, P.; Lee, J.; Angelova, L.V.; Ormsby, B. Reviving WHAAM! a comparative evaluation of cleaning systems for the conservation treatment of Roy Lichtenstein’s iconic painting. *Herit. Sci.* **2020**, *8*, 9. [[CrossRef](#)]
14. Mastrangelo, R.; Chelazzi, D.; Poggi, G.; Fratini, E.; Pensabene Buemi, L.; Petruzzelis, M.L.; Baglioni, P. Twin-chain polymer hydrogels based on poly(vinyl alcohol) as new advanced tool for the cleaning of modern and contemporary art. *Proc. Natl. Acad. Sci. USA* **2020**, *117*, 7011–7020. [[CrossRef](#)]
15. Vigorelli, L.; Re, A.; Guidorzi, L.; Cavaleri, T.; Buscaglia, P.; Nervo, M.; Del Vesco, P.; Borla, M.; Grassini, S.; Lo Giudice, A. Multi-analytical approach for the study of an ancient Egyptian wooden statuette from the collection of Museo Egizio of Torino. *Acta Imeko* **2021**, in press.
16. Petrakakis, K.; Dietrich, H. MINSORT: A program for the processing and archivation of microprobe analysis of silicate and oxide minerals. *Neues Jb. Miner. Abh.* **1985**, *8*, 379–384.
17. Lo Giudice, A.; Re, A.; Angelici, D.; Corsi, J.; Gariani, G.; Zangirolami, M.; Ziraldo, E. Ion microbeam analysis in cultural heritage: Application to lapis lazuli and ancient coins. *Acta Imeko* **2017**, *6*, 76–81. [[CrossRef](#)]
18. Oleari, C. *Misurare il Colore*, 2nd ed.; Hoepli: Milano, Italy, 2008; pp. 222–224, ISBN 8-820-34126-3.
19. Piquette, K.E. Reflectance transformation imaging (RTI) and Ancient Egyptian material culture. *Damqatum CEHAO Newsl.* **2011**, *7*, 16–20.
20. Serotta, A. An investigation of tool marks on Ancient Egyptian hard stone sculpture: Preliminary report. In *Metropolitan Museum Studies in Art, Science, and Technology*; Centeno, S.A., Kennedy, N.W., Manuels, M., Schorsch, D., Stone, R.E., Sun, Z.J., Wypyski, M.T., Eds.; Metropolitan Museum of Art: New York, NY, USA, 2014; Volume 2, pp. 197–201, ISBN 0-300-20439-6.
21. Wolbers, R. *Cleaning Painted Surfaces: Aqueous Methods*; Archetype Publications: London, UK, 2000; ISBN 978-1-873132-36-4.
22. Hatton, G.D.; Shortland, A.J.; Tite, M.S. The production technology of Egyptian blue and green frits from second millennium BC Egypt and Mesopotamia. *J. Archaeol. Sci.* **2008**, *35*, 1591–1604. [[CrossRef](#)]
23. Scott, D.A. A review of ancient Egyptian pigments and cosmetics. *Stud. Conserv* **2016**, *61*, 185–202. [[CrossRef](#)]
24. Pagès-Camagna, S.; Colinart, S. The Egyptian green pigment: Its manufacturing process and links to Egyptian blue. *Archaeometry* **2003**, *45*, 637–658. [[CrossRef](#)]

25. Asperger, A.; Engewald, W.; Fabian, G. Advances in the analysis of natural waxes provided by thermally assisted hydrolysis and methylation (THM) in combination with GC/MS. *J. Anal. Appl. Pyrolysis* **1999**, *52*, 51–63. [[CrossRef](#)]
26. Asperger, A.; Engewald, W.; Fabian, G. Thermally assisted hydrolysis and methylation—A simple and rapid online derivatization method for the gas chromatographic analysis of natural waxes. *J. Anal. Appl. Pyrolysis* **2001**, *61*, 91–109. [[CrossRef](#)]
27. Girod, A.; Weyermann, C. Lipid composition of fingerprint residue and donor classification using GC/MS. *Forensic Sci. Int.* **2014**, *238*, 68–82. [[CrossRef](#)] [[PubMed](#)]
28. Riedo, C.; Scalalone, D.; Chiantore, O. Advances in identification of plant gums in cultural heritage by thermally assisted hydrolysis and methylation. *Anal. Bioanal. Chem.* **2010**, *396*, 1559–1569. [[CrossRef](#)] [[PubMed](#)]
29. Riedo, C.; Scalalone, D.; Chiantore, O. Multivariate analysis of pyrolysis-GC/MS data for identification of polysaccharide binding media. *Anal. Methods* **2013**, *5*, 4060–4067. [[CrossRef](#)]
30. Daniels, V.; Stacey, R.; Middleton, A. The blackening of paint containing Egyptian blue. *Stud. Conserv.* **2004**, *49*, 217–230. [[CrossRef](#)]
31. Challinor, J.M. Characterisation of wood by pyrolysis derivatisation-gas chromatography/mass spectrometry. *J. Anal. Appl. Pyrolysis* **1995**, *35*, 93–107. [[CrossRef](#)]
32. Buckley, S.A.; Evershed, R.P. Organic chemistry of embalming agents in Pharaonic and Graeco-Roman mummies. *Nature* **2001**, *413*, 837–841. [[CrossRef](#)] [[PubMed](#)]
33. Fabbri, D.; Chiavari, G.; Galle, G.C. Characterization of soil humin by pyrolysis(/methylation)-gas chromatography/mass spectrometry: Structural relationships with humic acids. *J. Anal. Appl. Pyrolysis* **1996**, *37*, 161–172. [[CrossRef](#)]
34. Kaal, J.; Nierop, K.G.J.; Kraal, P.; Preston, C.M. A first step towards identification of tannin-derived black carbon: Conventional pyrolysis (Py-GC-MS) and thermally assisted hydrolysis and methylation (THM-GC-MS) of charred condensed tannins. *Org. Geochem.* **2012**, *47*, 99–108. [[CrossRef](#)]
35. Chiavari, G.; Montalbani, S.; Prati, S.; Keheyan, Y.; Baroni, S. Application of analytical pyrolysis for the characterisation of old inks. *J. Anal. Appl. Pyrolysis* **2007**, *80*, 400–405. [[CrossRef](#)]
36. Guidotti, C.V. Micas in metamorphic rocks. *Rev. Mineral.* **1984**, *13*, 357–467.
37. Massone, H.J.; Schreyer, W. Phengite geobarometry based on the limiting assemblage with K-feldspar, phlogopite and quartz. *Contrib. Mineral. Petrol.* **1987**, *96*, 212–224. [[CrossRef](#)]
38. De Putter, T.; Karlshausen, C. *Les Pierres Utilisées dans la Sculpture et L'architecture de l'Égypte Pharaonique: Guide Pratique Illustré; Connaissance de l'Égypte Ancienne*: Bruxelles, Belgium, 1992; ISBN 2-87268-003-9.
39. Klitzsch, E.; Harms, J.C.; Lejal-Nicol, A.; List, F.K. Major subdivisions and depositional environments of Nubia strata, Southwestern Egypt. *Am. Assoc. Pet. Geol. Bull.* **1979**, *63*, 967–974. [[CrossRef](#)]
40. Finger, F.; Dörr, W.; Gerdes, A.; Gharib, M.; Dawoud, M. U-Pb zircon ages and geochemical data for the Monumental Granite and other granitoid rocks from Aswan, Egypt: Implications for the geological evolution of the western margin of the Arabian Nubian Shield. *Mineral. Petrol.* **2008**, *93*, 153–183. [[CrossRef](#)]
41. Borghi, A.; Vaggelli, G.; D'Amicone, E.; Fiora, L.; Maschali, O.; Shalaby, B.; Vigna, L. Bekhen stone artifacts in the Egyptian Antiquity Museum of Turin (Italy): A mineropetrographic study. In Proceedings of the 2nd International Conference on the Geology of the Tethys, Cairo University, Cairo, Egypt, 19–22 March 2007.
42. Lee, L.; Quirke, S. Painting materials. In *Ancient Egyptian Materials and Technology*; Nicholson, P.T., Shaw, I., Eds.; Cambridge University Press: Cambridge, UK, 2000; pp. 104–120, ISBN 0-521-12098-5.